sented here, is necessary for a rigorous understanding of fundamental many-body interactions.

In the following, we analyze the low-fluence data shown in Fig. 1 (a) with the microscopic theory outlined above. The free parameters are the exciton Rydberg energy E_R, the exciton dephasing γ_2, and the decay rate of the biexciton amplitude γ_b. We show in Fig. 1 (b) our theoretical results for an optimized value of γ_b, which is $\gamma_b = \gamma_2/3$. In Fig. 1 (c) we show results obtained for $\gamma_b = 2\gamma_2$, a value often believed appropriate for most experimental conditions.

While unavoidable experimental fluctuations prevent us from claiming that the true value for γ_b is exactly $\gamma_2/3$, we do believe that our analysis gives strong evidence for reduced biexciton dephasing under the conditions of our experiment. Furthermore, we note that theoretical results without coherent-biexciton and two-exciton continuum correlations (not shown) do not yield good agreement.

In summary, the microscopic many-body theory applied to the time-resolved vectorial polarization state of the FWM signal documents two-exciton correlations. Under our experimental conditions, the biexciton dephasing rate is found to be much less than twice the exciton dephasing rate.

This work is supported by NSF (DMR).

References

1. A.E. Paul, J.A. Bolger, A.L. Smirl, and J.G. Pellegrino, J. Opt. Soc. Am. B 13, 1016 (1996).
2. For a review see A.L. Smirl, in *Semiconductor Quantum Electronics: From Quantum Physics to Smart Devices,* edited by A. Miller, M. Ebrahimzadeh, and D.M. Finlayson (IOP Publishing, Bristol, 1974), pp. 25–93.
3. B. Haase *et al.*, Phys. Rev. B 59, 7805 (1999).
4. V.M. Axt and A. Stahl, Z. Phys. B 93, 195 (1994).
5. W. Schäfer and M. Wegener, *Semiconductor Optics and Transport Phenomena—from fundamentals to current topics* (Springer, Berlin, 2002), to be published.
6. R. Binder, I. Rumyantsev, N.H. Kwong, and R. Takayama, Phys. Stat. Sol. (b) 221, 169 (2000).
7. N. Kwong, R. Takayama, I. Rumyantsev, M. Kuwata-Gonokami, R. Binder, Phys. Rev. Lett. 87, art. no. 027402 (2001).

QThF5 **11:15 am**

Observation of Coherent Acoustic Phonon Lasing in InGaN/GaN MQWs

Yue-Kai Huang, Gia-Wei Chern, and Chi-Kuang Sun, Graduate Institute of Electro-Optical Engineering, National Taiwan University, Taipei, 10617 Taiwan, R.O.C., Email: sun@cc.ee.ntu.edu.tw.

Stacia Keller and Steven P. DenBaars, Department of Electrical and Computer Engineering, University of California, Santa Barbara, CA 93106

One of the most desirable properties of phonon system is sound amplification by stimulated emission of phonon radiation, coined as SASER or called "phonon laser" or "acoustic laser", which is the acoustic counterpart of LASER. Phonon stimulated emission, or sound amplification, has been previously observed for several occasions[1,2] in extremely low temperatures, however a "lasing" behavior of the phonon oscillators has never been established. It is also desirable to build a phonon laser operating at room temperature. Here we present an exciting observation of the coherent acoustic phonon lasing behavior in InGaN/GaN MQWs.[3] InGaN/GaN MQWs behaved as a phononic-crystal distributed-feedback cavity thus only the specific phonon modes with its wavelength matching the MQWs period width could be selected for its coherent output. By using femtosecond ultraviolet pulses as pumping sources, coherent acoustic phonon amplification with over-10 dB acoustic gain was measured. When the induced acoustic gain is higher than the acoustic loss due to its acoustic traveling nature, a clear laser-like threshold behavior was observed.

Figure 1 shows an example of the interferometric measurement we used to study the acoustic gain in a coherent acoustic phonon oscillator. UV pump and amplification pulses, with time-delay T, were focused into the InGaN/GaN MQWs.[4] Resulted sample transmission change was then measured using femtosecond pump-probe technique. Fig. 1 is a differentiated probe transmission change as a function of time, where the induced coherent acoustic phonon oscillation period is 1.38 ps. Series of similar interferometric measurements were performed. Figure 2 shows a typical oscillation magnitude and phase variation as a function of time-delay T between two interfered pulses. With the lattice displacing force being proportional to the photo-excited carrier density,[3] the final oscillation after the interference should simply be the linear superposition of the oscillations induced by the two pulses. Nevertheless, a linear fitting curve (dotted-lines in Fig. 2) simply could not match the observed results, which differed dramatically in phase at destructive interference and in amplitude at constructive interference. A calculation assuming phononic gain on the initial oscillation had much better resemblance. Thus obtained amplification ratio for Figure 2 was 1.7, which would give a 4.6 dB acoustic gain. Other experiments suggested that acoustic gain increases linearly with the photoexcited carrier density. Large acoustic gain over 10 dB at room temperature was easily obtained with high excitation carrier density.

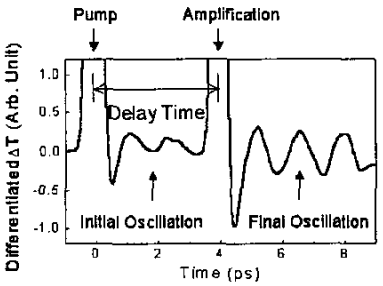

QThF5 Fig. 1. Differentiated probe transmission change vs. time delay in the amplification process. The excitation wavelength was 390 nm. The optical fluence ratio between the amplification pulse and the pump pulse is 1.16 with their pulse fluence being 6.3×10^{12} J/cm^2 and 5.4×10^{-5} J/cm^2.

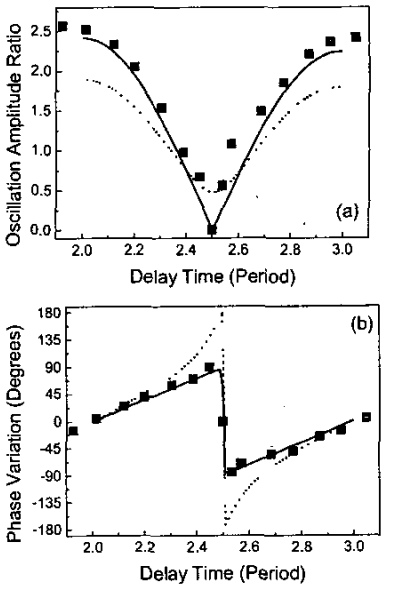

QThF5 Fig. 2. (a) Magnitude and (b) phase variations of the initial coherent phonon oscillation after the interferometric measurement as a function of pulse delay, from 2 to 3 oscillation periods. The 2D excited carrier density ratio of the two pulses are 4.3×10^{12} cm^{-2} (pump) and 4.9×10^{12} cm^{-2} (amplification). The squares are experimental data. The solid fitting curves represent system with acoustic gain 4.6 dB (G = 1.7) while dashed curves represent the one without acoustic gain (G = 1).

With such a large acoustic gain, phonon lasing threshold behavior can be observed by compensating the phonon system loss in one single huge pulse. To avoid destructive interference inside the pulse, the pulse width must be shorter than half of the oscillation period. Fig. 3 shows the observed coherent acoustic phonon oscillation intensity as a function of pulse-induced 2D photo-carrier density when we excited with one ~200 fs UV pulse. A clear lasing threshold behavior was observed with a threshold carrier density around 7×10^{12} cm^{-2}, corresponding to 6.5 dB acoustic

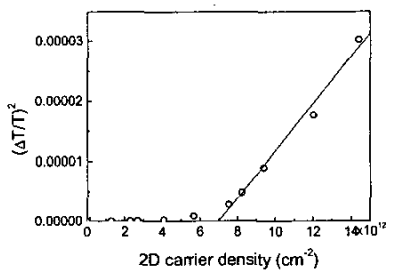

QThF5 Fig. 3. The relation between photo-excited density and the intensity of the induced coherent acoustic phonon waves in a 50/43 Å InGaN/GaN MQW (the intensity is proportional to the square of the oscillation amplitude, which is proportional to the transmission modulation). A threshold carrier density is identified around 7×10^{12} cm^{-2}.

loss. These results unveil the promising future of SASER, operating at pretersonic frequency and under room temperature, with a wavelength shorter than 10 nm. Detailed amplification and loss mechanism will also be discussed.

References

1. W.J. Brya and P.E. Wagner, "Dynamic Interaction between Paramagnetic Ions and Resonant Phonons in a Bottlenecked Lattice", Phys. Rev. 157, pp. 400–410 (1967).
2. L. Challis & S. Clough, "Hearing through a glass brightly", Nature 367, 687–688 (1994).
3. C.-K. Sun *et al.*, "Coherent Acoustic Phonon Oscillations in Semiconductor Multiple Quantum Wells with Piezoelectric Fields", Phys. Rev. Lett. 84, 179–182 (2000).
4. C.-K. Sun *et al.*, "Coherent Optical Control of Acoustic Phonon Oscillations in InGaN/GaN Multiple Quantum Wells", Appl. Phys. Lett. 78, 1201–1203 (2001).

QThF6 **11:30 am**

Strong Mid-Infrared Transient Absorption of One-dimensional Copper Oxide Sr_2CuO_3

M. Ashida, Exploratory Research for Advanced Technology, Japan Science and Technology Corporation, KSP D-842, 3-2-1 Sakato Takatsu-ku Kawasaki, 213-0012, Japan

S. Uchida, Y. Tokura, M. Kuwata-Gonokami, Department of Applied Physics, University of Tokyo, Tokyo 113-8656, Japan, gonokami@ap.t.u-tokyo.ac.jp

Electron correlation effects, which have attracted much interest after the discovery of high temperature superconductivity and manifest themselves in anomalous transport and/or magnetic phenomena, can also be found in optical properties of strongly correlated electron systems. In particular, we have recently discovered strong optical nonlinearity of one-dimensional (1D) Mott insulator Sr_2CuO_3 in near-infrared (IR) region.[1] Importantly, the material shows picosecond recovery of the optical transparency making it possible to employ this material in ultrafast all-optical switching devices.[2] However, the relaxation dynamics of the optical excited states is still unclear. To investigate the relaxation process, we performed pump-probe transmission measurements in mid- and near-IR region of 0.1–1 eV. We have found anomalously strong transient absorption band at 0.3 eV.

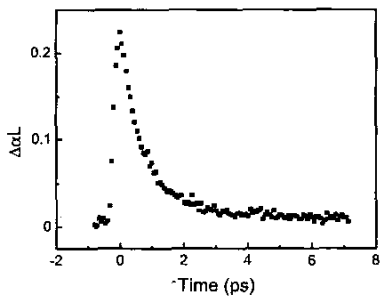

QThF6 Fig. 1. Temporal behavior of the $\Delta\alpha L$ in S r_2CuO_3 at 290 K. $\omega_{pump} = 1.6$ eV, $\omega_{probe} = 0.3$ eV.

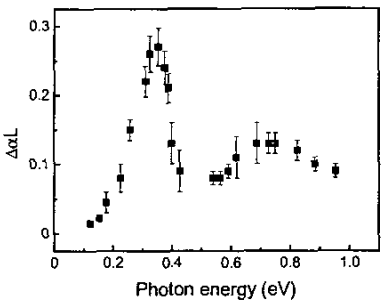

QThF6 Fig. 2. Transient absorption spectrum in Sr_2CuO_3 at 290 K. $\omega_{pump} = 1.6$ eV.

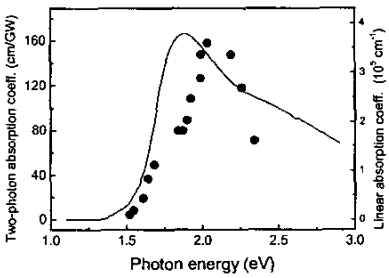

QThF6 Fig. 3. One-photon absorption (line) and two-photon absorption (circle) spectra in Sr_2CuO_3 at 290 K.[2]

We used two optical parametric oscillators pumped with a kHz regenerative amplifier to change the pump and the probe energies independently. Using differential frequency and second harmonic generation, we obtained 0.1–3 eV light pulses with ~0.2 ps width. Sample thickness L was 50–100 μm.

The photo-induced change of the absorption coefficient $\Delta\alpha$ was observed in the overall IR region from 0.1 to 1 eV at the pump photon energy $\omega_{pump} \geq 1.6$ eV, which corresponds to the absorption band of this material (see Fig. 3). A typical temporal behavior of the $\Delta\alpha L$ is shown in Fig. 1. The profile does not depend on the probe photon energy ω_{probe} in our experimental conditions. The transient absorption decays exponentially with time constant of ~1 ps, which is comparable with that we have measured at $\omega_{pump} < 1.6$ eV.[1]

The dependence of the instantaneous pump-induced absorption change on ω_{probe} is presented in Fig. 2. One can see that this transient absorption spectrum consists of a relatively sharp band at 0.3 eV and a broader band centered at 0.7 eV. This spectral profile does not depend on ω_{pump}, indicating that the optical excited state is instantaneously relaxed within the one-photon band, i.e. the IR photon probes the transition between the relaxed state of the one-photon manifold and different even parity states. One can observe from Fig 3 that the position of the sharp band in the transition absorption spectrum coincides with the energy difference between the one- and two-photon absorption bands.[1,2] Therefore, the band at 0.3 eV corresponds to the transition from the relaxed one-photon state to a two-photon state. Since the measured absorption cross section of this transition is found to be two times larger than that of the one-photon transition at 1.8 eV in Fig. 3, the dipole coupling between the relaxed excited states is one-order of magnitude larger than that between the ground and one-photon states. This is consistent with our results on the enhanced dipole coupling between the excited states of different parity in Sr_2CuO_3.[1]

The broader band centered at 0.7 eV in Fig. 2 may be attributed to the sideband of the sharp band at 0.3 eV. This sideband is associated with the spin excited states (spinons), which exist in Sr_2CuO_3 due to the large antiferromagnetic coupling between neighboring Cu sites with large exchange energy $J \sim 0.2$ eV.[3] The appearance of the spinon sideband in the transient absorption spectrum indicates that the spin degree of freedom is crucial for the relaxation process in this material.

References

1. T. Ogasawara, M. Ashida, N. Motoyama, H. Eisaki, S. Uchida, Y. Tokura, H. Ghosh, A. Shukla, S. Mazumdar and M. Kuwata-Gonokami, Phys. Rev. Lett. 85, 2204 (2000).
2. M. Ashida, T. Ogasawara, Y. Tokura, S. Uchida, S. Mazumdar and M. Kuwata-Gonokami, Appl. Phys. Lett. 78, 2831 (2001).
3. H. Suzuura, H. Yasuhara, A. Furusaki, N. Nagaosa, and Y. Tokura, Phys. Rev. Lett. 76, 2579 (1996).

QThF7 **11:45 am**

Coupled Bloch-phonon Oscillations in Biased InGaAs/InAlAs Superlattices

M. Först and H. Kurz, Institut für Halbleitertechnik, RWTH Aachen, Sommerfeldstr. 24, D-52074 Aachen, Germany, Email: foerst@iht-ii.rwth-aachen.de

T. Dekorsy, Institut für Ionenstrahlphysik und Materialforschung, Forschungszentrum Rossendorf, D-01314 Dresden, Germany

R.P. Leavitt, U.S. Army Research Laboratory, 2800 Powder Mill Road, Adelphi, Maryland 20783

Recently, the coupling of coherent Bloch oscillations and longitudinal optical (LO) phonons has been studied experimentally and theoretically in $GaAs/Al_{0.3}Ga_{0.7}As$ superlattices with minibands larger than the phonon energy.[1,2] When the Bloch oscillations are tuned in resonance with the GaAs LO phonon frequency, the coherent excitation of the LO phonon was observed due to the coupling via the associated longitudinal electric fields. The excitation of the AlAs-like LO phonon corresponding to the barriers could not be observed.

In this paper, we present experimental results on coupled Bloch-phonon oscillations in a ternary $In_{0.53}Ga_{0.47}As/In_{0.52}Al_{0.48}As$ superlattice grown lattice-matched on InP. The well and barrier thicknesses are 8.4 and 51.6 Å, respectively, leading to a first electronic miniband of 60 meV width that is weakly confined. This miniband width enables the coherent optical excitation of Bloch oscillations that are tunable above the LO phonon frequencies of both superlattice barriers and wells. The coherent polarizations of the coupled carrier and lattice dynamics are detected via a time-resolved electro-optic sampling technique (REOS)[3] using 45 femtosecond pulses from a Ti:Sapphire oscillator.

To coherently excite Bloch oscillations, the laser source was tuned to a wavelength of 890 nm thus superposing adjacent electronic Wannier-Stark states, i.e. the WS(0) and WS(−1) states, in